Preprints (www.preprints.org) | NOT PEER-REVIEWED | Posted: 23 September 2020 doi:10.20944/preprints202009.0528.v1

Elemental Micro-characteristic, Thermogravimetric, and FTIR study of Green Sand(Poly Lactic Acid) for replacement of Fine Aggregate in Concrete Mix

Arun Y Patil[1], N R Banapurmath[2], Sumukh E P[3], Manojkumar V Chitawadagi[4], Yunuskhan T M[5], Irfan Anjum Badruddin[6], Sarfaraz Kamangar[7]

[1,2,5,6,7]School of Mechanical Engineering, [3,4] School of Civil and Environmental Engineering B.V.B. College of Engineering and Technology, KLE Technological University, Hubli, India.

[5,6,7]Research Centre for Advanced Material Science(RCAMS), King Khalid University, Saudi Arabia

Corresponding author: patilarun7@gmail.com

Graphical Abstract:

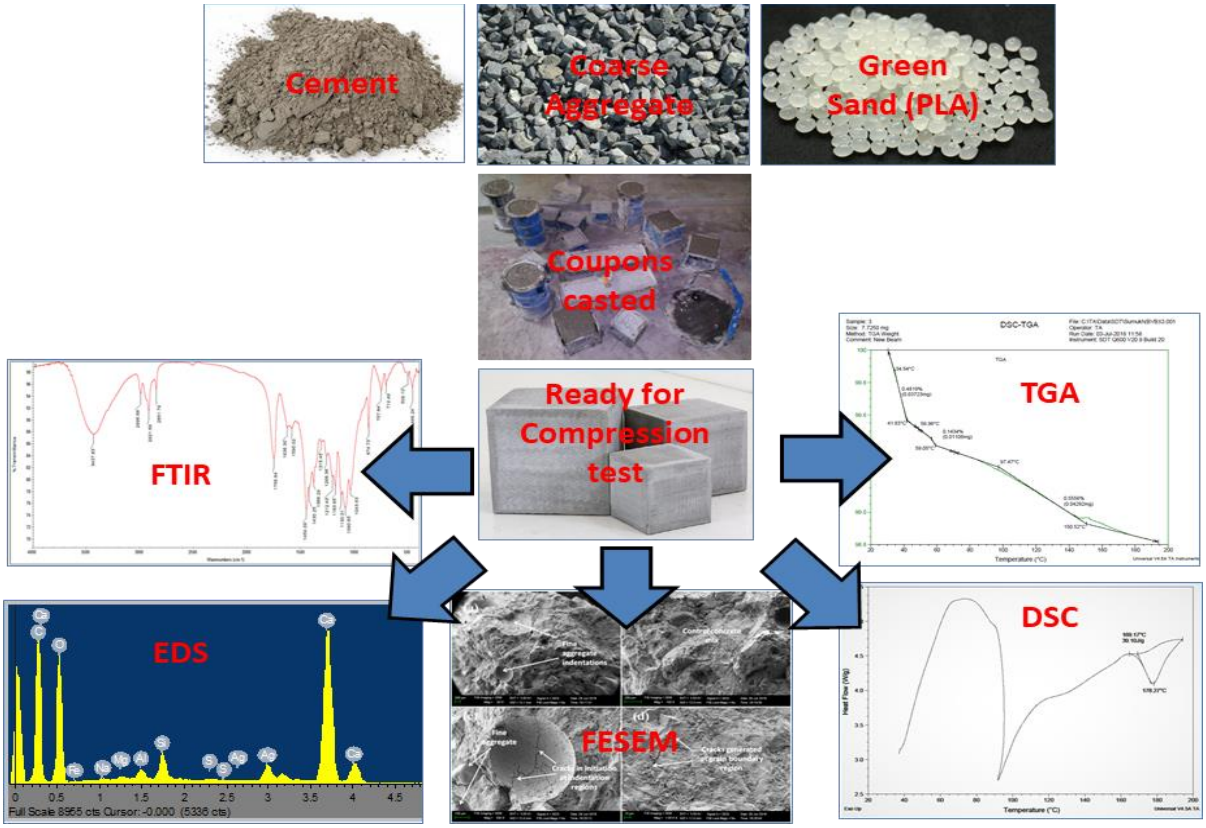

Abstract

Poly lactic acid (PLA) has made inroads for commercial market segment with lot many unique characteristics such as tenacity, low flame rate, moisture regain percentage, loss of ignition percentage, heat of combustion, UV resistance, Elastic recovery and higher melting point allowed it to be the fastest moving material in today's commercial market. An attempt has been made to test the feasibility and biocompatibility aspect of PLA with cement mix.

 doi:10.20944/preprints202009.0528.v1

The basic strength and physical test results were carried out and published in an article, to the continuation of the work, micro-structural study was conducted to evaluate the elemental characteristics. Thermo gravimetric analysis revealed that PLA either in granular form or filament will hold good for the inclusion into construction applications, provided degradation aspects are to be looked out for improvisation. From DSC it was found that PLA in filament form is the best inclusion material for construction application, however the tenacity of fibers has to checked, as currently available filaments in market does not have high tenacity value. From EDX reports, 30% inclusion of PLA as replacement for fine aggregate has constituent members as Calcium carbonate($CaCO_3$), Silica(SiO_2) and Wollastonite (CaK) resulted in best composition among the rest. FESEM images revealed that, proper gradation in size, rough surface of PLA granular form or filament form will definitely enhance the mechanical/physical or even chemical behavior of PLA.

Keywords: Poly Lactic Acid(PLA), TGA, FTIR, DSC, FESEM, EDX.

1. Introduction

As per plastic insight[1], by 2020 global poly lactic acid(PLA) market will reach a milestone of more than US$ 5billion. Currently the usage has cater to many diversified domains such as Medical, Food packaging, Textile, Agricultural, Consumer electronics, personal care etc. As in India, still the usage is limited to 1% of global utilization in 2015[2]. Solid waste generation in India has opened a Pandora of opportunity boxes to recycle the dry solid waste with best outputs.

Today, material characterization has become part of research, for identifying the critical parameters such as micro/nano structural study with the help of SEM/FESEM/TEM, loss of volatile components viz. moisture, solvent and monomers, decomposition, noticing the residue composition using TGA, Enthalpy, melting point and specific heat capacity by DSC, to arrive at an infrared spectrum of absorption or emission of all three phases such as a solid, liquid or gaseous material using FTIR. Current generation TGA DSC has wide range of measurement techniques, can be performed dynamically using a linear temperature ramp or isothermally[3]. Temperature ramps are used to investigate the temperature dependents and process such as loss of moisture, composition and chemical reaction. Isothermal measurements are mainly used to determine the oxidation induction time of material or to study the release or absorption of moisture. The atmosphere often switched from inert to oxidative to burn the carbon black or determine the ash or filler content. Measurements under

Preprints (www.preprints.org) | NOT PEER-REVIEWED | Posted: 23 September 2020 doi:10.20944/preprints202009.0528.v1

reduced pressure or vacuum are employed to separate overlapping effect of vaporization and decomposition. Simultaneously measured DSC signal records exothermic and endothermic events such as the Glass Transition Temperature(GTT), melting, crystallization, chemical reaction and phase transitions.

2. Characterization Study

2.1 Thermo gravimetric analysis (TGA)

Thermo gravimetric analysis (TGA) measures loss of mass of a sample when it is subjected to heat, cool or constant temperature. It represents the mass loss curve, in which abscissa illustrates temperature in degree Celsius and ordinate with weight percentage. The weight loss of coupon subjected to TGA is established via Five major steps. In first step, loss of volatile components such as moisture, monomers and solvents. Second step focuses on decomposition of specimen, in third step atmosphere switched from Nitrogen to Oxygen. Fourth step is to combustion of carbon in endothermic or exothermic condition. Finally, inert inorganic residue of ash fillers. Aluminium crucibles were used to hold the specimens and working temperature of upto 600°C. The characterization was applied to PLA in granular form, PLA in filament form and PLA in wafer form derived from degradation of matrix in concrete mortar.

2.1.1 PLA granules: PLA granules were procured from Nature works, USA. The figure 1 depicts the shape and aesthetic appeal of granules. The granules are embedded in concrete mix at a proportion of 0%, 10%, 30% and 50% volume fraction of PLA as a replacement for fine aggregate.

Fig 1. PLA granules

PLA as a polymeric material often contains small amounts of carbon black for coloration and stabilization. The carbon black content can be determined by switching to a reactive gas after pyrolysis of the polymer. The example shows the analysis of a poly lactic acid sample in

Preprints (www.preprints.org) | NOT PEER-REVIEWED | Posted: 23 September 2020 doi:10.20944/preprints202009.0528.v1

granule form with 7.725 mg. From figure 2, TGA curve can be divided into four steps. In first, upto 41.83°C loss of volatile components such as moisture solvent and monomers. Decomposition of PLA carbon and its allied members at 59.05°C in step 2. The third step atmosphere switched from Nitrogen to Oxygen, to cater for combustion of carbon in next step. Finally resulting into inert inorganic residue of ash fillers or other impurities. Evaluation of a pyrolysis weight loss step yields a polymer content of 98.8%, as a result 1.2% weight loss was achieved for granular form.

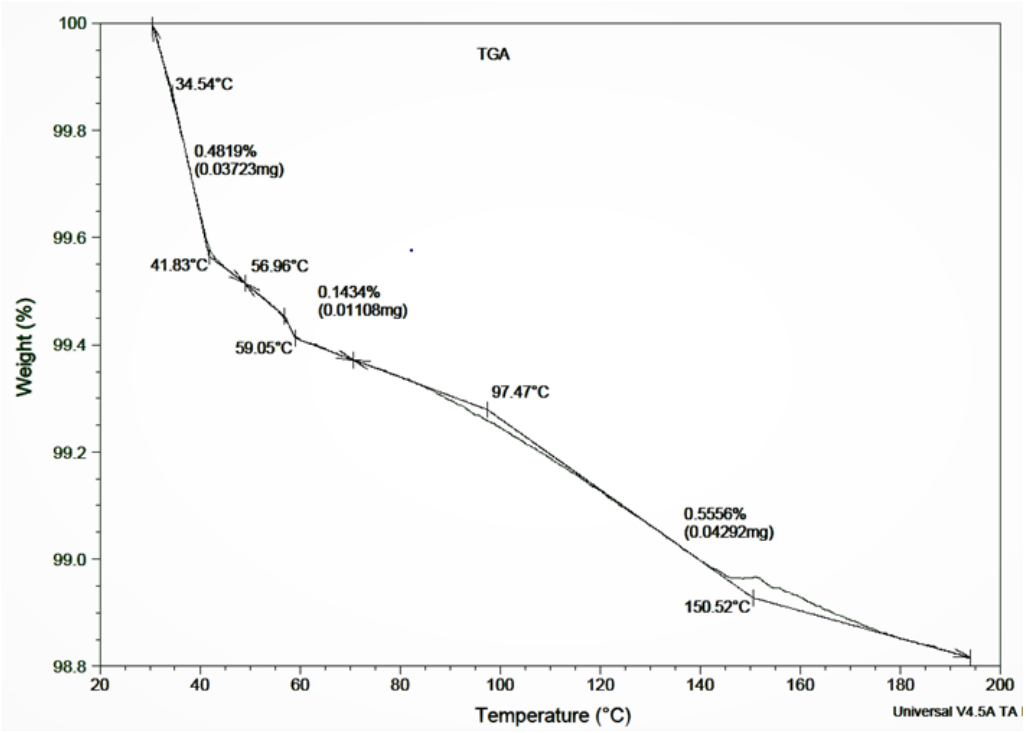

Fig 2. Weight loss vs. Temperature curve for PLA granules

2.1.2 PLA in filament(wired) form:

PLA in its filament(wired) form was extruded to use for 3D printing applications. When the same is subjected to TGA resulted with comparatively less amount of carbon black percentage(approximately 1%), in figure 3 shows that minimal amount of impurity. Temperature ramps are used to measure temperature dependent process such as loss of moisture, composition and chemical reaction. PLA in wired form weighing about 5.013 mg was heated at a heating rate of 10°C/min from 20°C to 200°C. The glass transition point T_g and melting point T_m was measured.

2.1.3 Reacted layer on PLA granules:

As depicted in Figure 4, PLA in its diaphragm or wafer form does subjected to chemical reaction with concrete mortar for 28 days of curing. When the coupon tested at 7 days time

Preprints (www.preprints.org) | NOT PEER-REVIEWED | Posted: 23 September 2020 doi:10.20944/preprints202009.0528.v1

limit, there was no sign of degradation in its outer peels of PLA granule but full cured sample yielded with white layer in the form of wafer. The wafer, as shown in figure 5 reveals that, entire process of moisture desorption and decomposition carried out in two steps. The percentage of mass loss observed was 25% yielding as expected 75% before it flattens with respect to abscissa measure with temperature at 200°C. Among the three cases, it is interesting to know further like what parameters caused the weight loss of PLA and any chemical reaction with cement mortar or water soaking (submerging in water) to convert an hydrophilic to hydrophobic are the areas of interest. To know and analyze on these issues the layer was subjected to FT-IR & DSC tests.

Reacted PLA layer degrades in three stages. The first stage (23.52°C – 40.89 °C) is due to the, loss of surface water and di-hydroxylation of the material with a weight loss of 0.93% in this period. The second transition (40.89°C – 100.82 °C) is related to the degradation of cellulosic substances such as hemicelluloses and cellulose with a weight loss of 21.06%. The third stage (100.82 – 120 °C) of the decomposition is due to the degradation of non-cellulosic materials with a weight loss of 0.863%. From 120 °C onwards, the relationship between weight and temperature is almost linear.

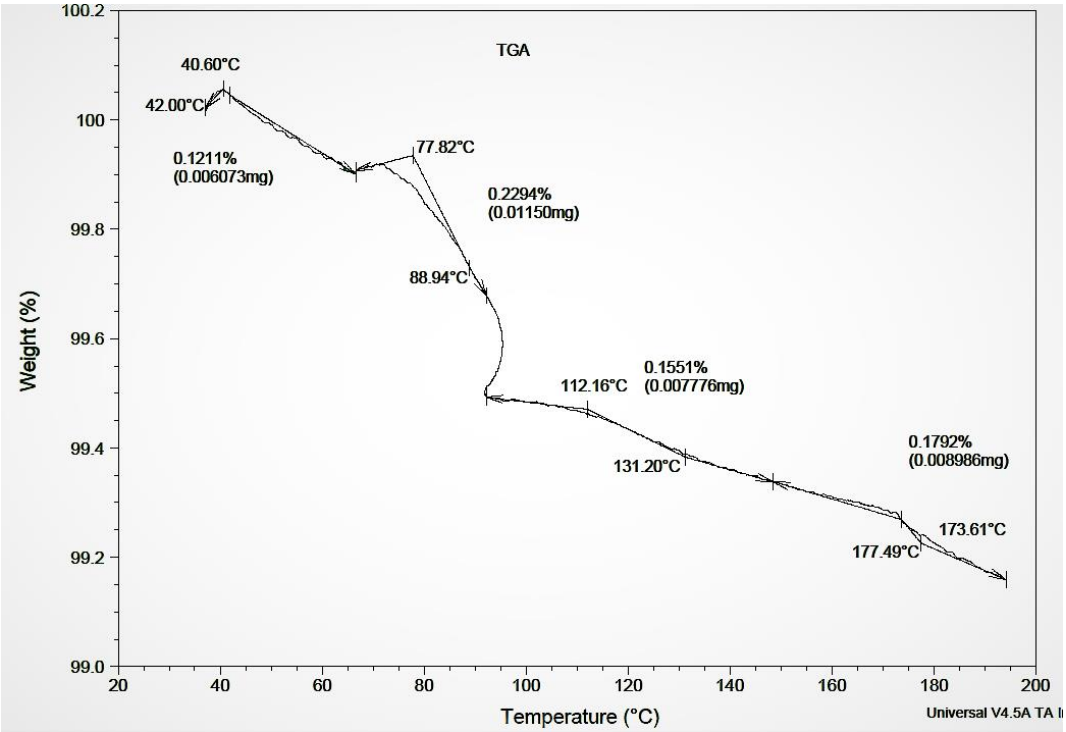

Fig 3. Weight loss vs. Temperature curve for wired PLA

Preprints (www.preprints.org) | NOT PEER-REVIEWED | Posted: 23 September 2020 doi:10.20944/preprints202009.0528.v1

Fig 4. PLA outer layer (wafer or diaphragm) formed during curing period.

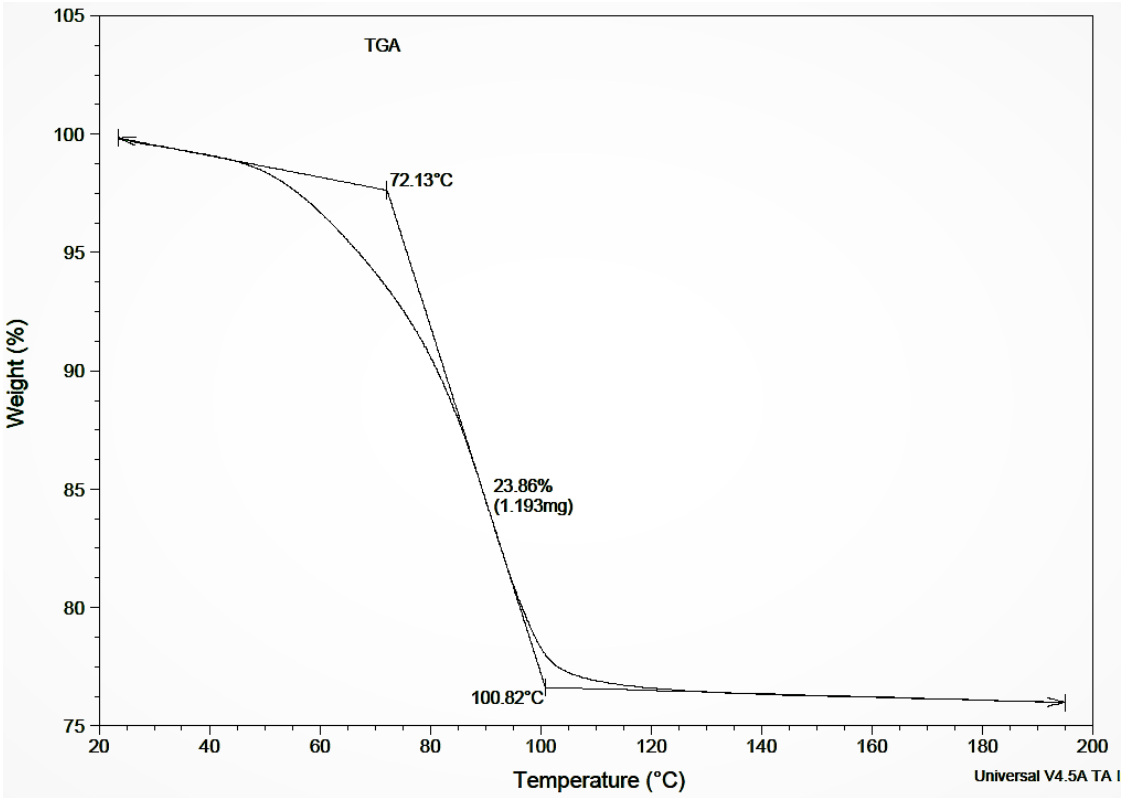

Fig 5. Weight loss vs. Temperature curve for reacted PLA layer

2.2 Differential scanning calorimetry (DSC)

Preprints (www.preprints.org) | NOT PEER-REVIEWED | Posted: 23 September 2020 doi:10.20944/preprints202009.0528.v1

DSC is a thermo analytical method. It is used to study the behavior of material as a function of temperature or time. Melting point, crystallization behavior and chemical reaction are just some of the many properties or processes that can be measured by DSC[3]. It measures the energy when subjected to heat, cool or held at isothermal condition. The respective samples may undergo one or more phase changes during heating or cooling. These changes are called "thermal transitions" of a polymer. Examples of the thermal transitions are glass transitions, crystallization, and melting of a polymer.

In the polymer field it is important to know the temperature range in which the polymers stable and in range which polymer decomposition occurs. DSC provides an information on purity of the sample if the stoichiometry of reaction is known. Results of isothermal and temperature ramped case can be used to determine the reaction kinetics. Other applications include the investigations of desorption or adsorption processes, evaporation behavior or influence of reactive gas. DSC applicable for evolved gas analysis of hyphenated techniques such as Mass spectrometry, FTIR.

Generally polymers behave in a significantly different manner when the temperature drops below T_g (more brittle) or goes up to higher temperatures than T_g (more rubbery). Hence to select a material for a specific application it is essential to know the behavior of composites under applied heat flow.

DSC measurements were conducted using a calibrated instrument available with a cooling attachment, in inert nitrogen atmospheric condition. Each samples were cut into tiny pieces (about 4 – 10 mg) and sealed in hermetic pans and lids. To build a reasonable reliability of the results, for each material three pieces of sample from different region were evaluated by DSC. The data were collected by repeated heating-cooling-heating cycles. The heating and cooling rate was 10 °C/min.

2.2.1 PLA granules

In this analysis, weight of sample taken was about 7.725 mg and the samples were heated up to 190 °C and held in a molten state for 5 min, followed by cooling down to 20 °C.

Glass transition temperature (Tg) = 54.04°C

Crystallization temperature (Tc) = 143.87°C

Melting temperature (Tm) = 154.15°C

Preprints (www.preprints.org) | NOT PEER-REVIEWED | Posted: 23 September 2020 doi:10.20944/preprints202009.0528.v1

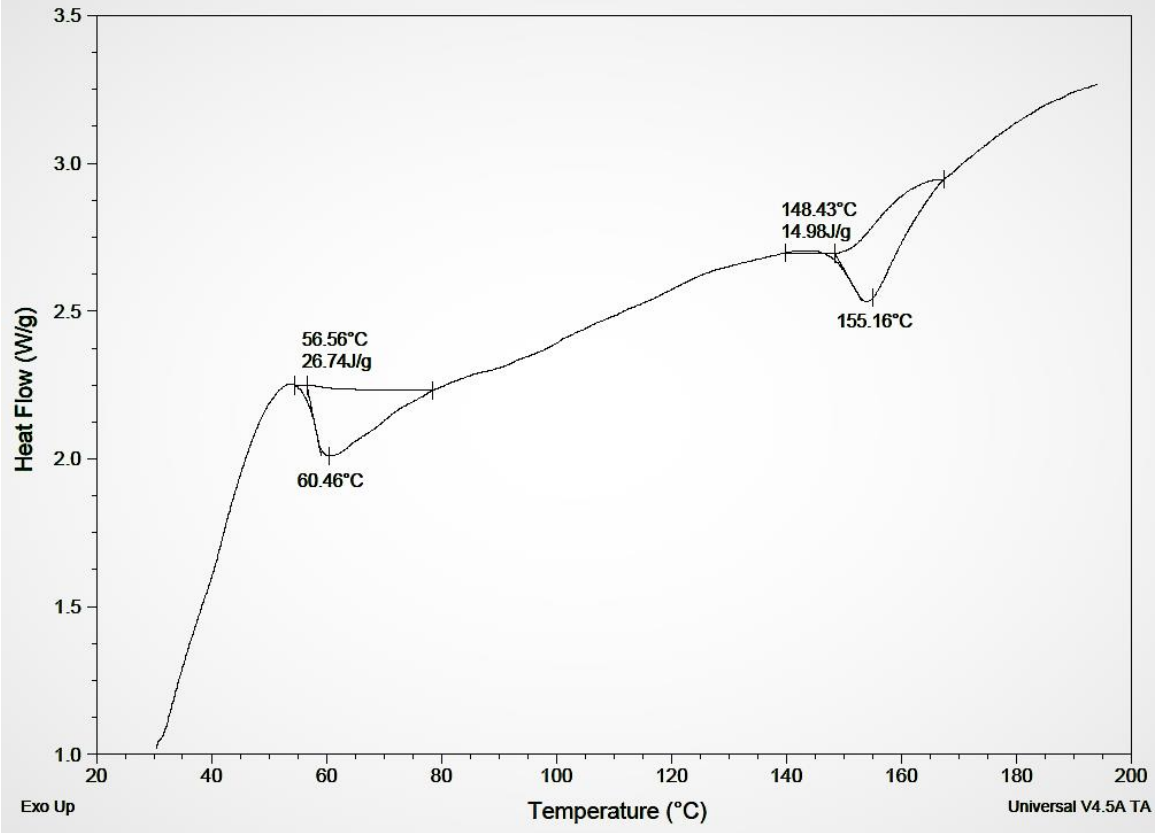

Fig 6. Heat flow vs. Temperature behaviour of PLA granules

2.2.2 PLA in wired form

From figure 7 a wired form of PLA was subjected to testing through TGA, resulting in a new pictorial representation of heat flow compared to granular form. The reason might be due to decomposition of chemical bond termination[4].

In this analysis, weight of sample taken was about 5.013 mg and the samples were heated up to 190 °C and held in a molten state for 5 min, followed by cooling down to 20 °C.

Glass transition temperature (Tg) = 76.03°C

Crystallization temperature (Tc) = 165.09°C

Melting temperature (Tm) = 177.94°C

Preprints (www.preprints.org) | NOT PEER-REVIEWED | Posted: 23 September 2020 doi:10.20944/preprints202009.0528.v1

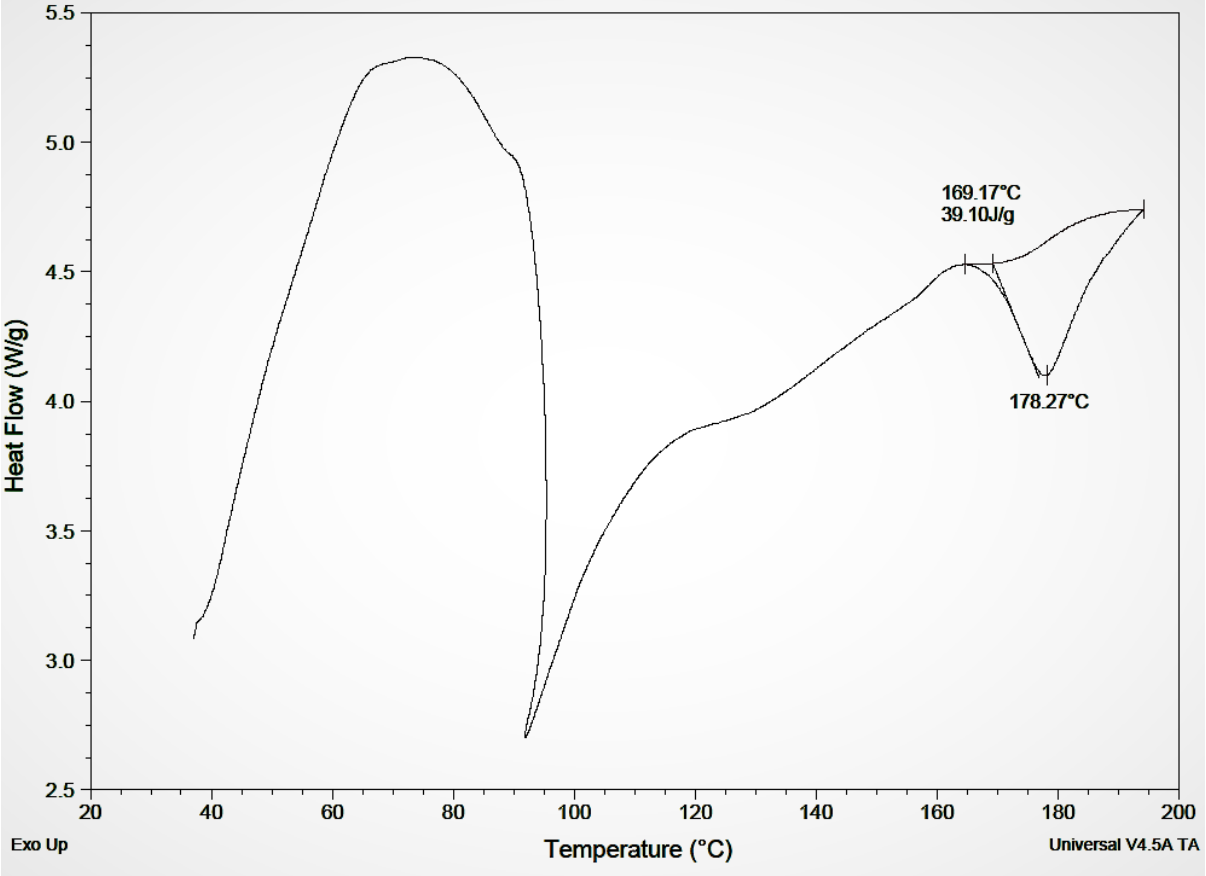

Fig 7. Heat flow vs. Temperature behavior of wired PLA

2.2.3 Reacted layer on PLA granules

From figure 8 it can be inferred that concentration of PLA as gets linked with cement an hydrolysis process delivers an early degradation of coupons. Higher the percentage of inclusion of PLA combination yields with less defensive and is characterized by decreased degradation temperature. This decrease in temperature result due to low bond strength and early decay of material[5].

In this analysis, weight of sample taken was about 4.999 mg and the samples were heated up to 190 °C and held in a molten state for 5 min, followed by cooling down to 20°C[6].

Glass transition temperature (Tg) = 48.11°C

Melting temperature (Tm) = 95.57°C

Preprints (www.preprints.org) | NOT PEER-REVIEWED | Posted: 23 September 2020 doi:10.20944/preprints202009.0528.v1

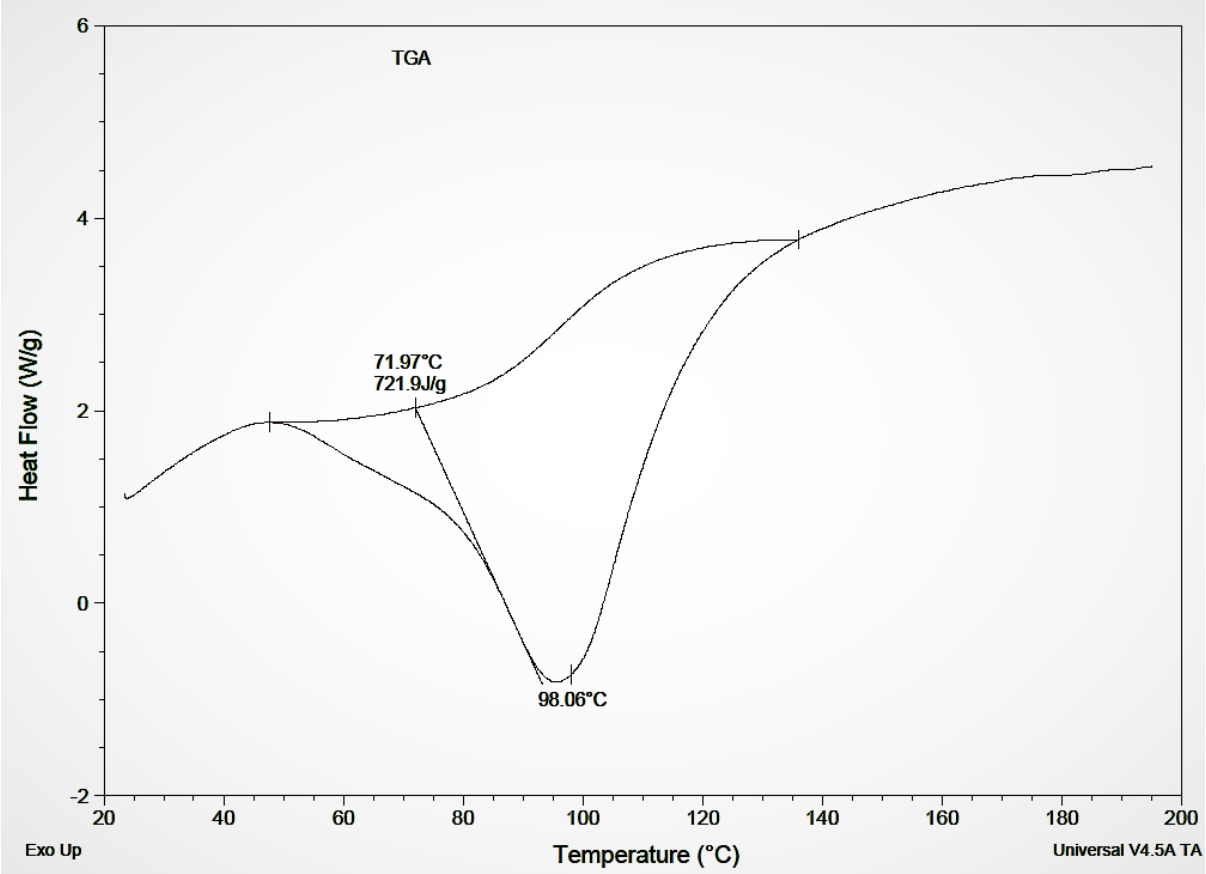

Fig 8. Heat flow vs. Temperature behaviour of reacted PLA layer

2.3 Fourier transform Infrared spectroscopy (FT-IR)

2.3.1 PLA Granules

The FTIR spectroscopy deals with the study of functional clusters such as PLA granules at various weight percentage inclusions to diagnose the effect of PLA with concrete and any chemical changes happening in the surrounding region of bonding. From figure 9 it can be inferred that, a broad peak of 3437 cm^{-1} was observed indicating a hydroxyl group with pristine sample subjected to testing with lesser lignin and hemicellulose content than wired filament form. The effect when compared with Kenaf fiber with treated 3324cm^{-1} and untreated 3318cm^{-1}[7]. Further the characteristics were compared with PLA, PLA/Kenaf (Untreated), PLA/Kenaf (Treated) and PLA/Kenaf (Treated) /EJO samples[7]. Bio composite coupon interpreting a combination of PLA and fibre mixing peak. Considering the fact that concrete will undergo hydration and calcinations process the expected result will definitely affect for combination of PLA and concrete coupon. However as for all three samples besides PLA spectrum, they had approximately similar wavelength as compared to PLA's except the difference in the peak intensity in the C=O stretching and C−O stretching for PLA.

Preprints (www.preprints.org) | NOT PEER-REVIEWED | Posted: 23 September 2020 doi:10.20944/preprints202009.0528.v1

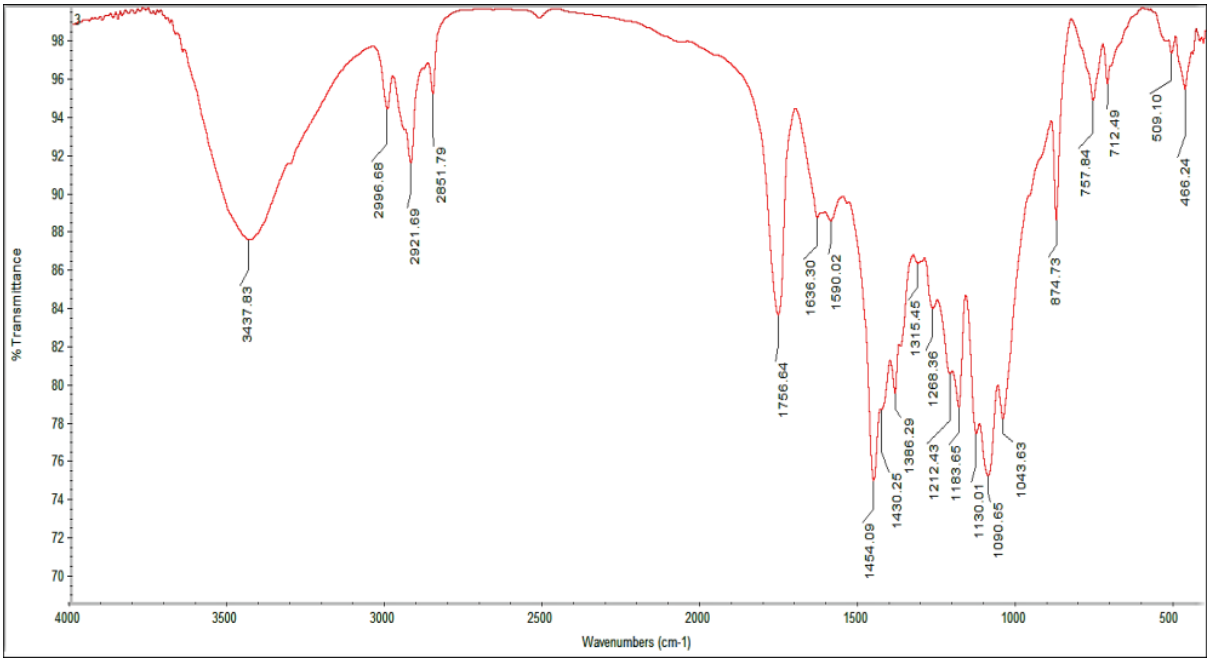

Fig 9. Characteristic bands in IR spectrum of PLA granules

Table 1. Characteristic peak positions in IR spectrum for PLA granules

Bonding	**Type**	**Characteristic peak positions (cm^{-1})**
-C-C-	Stretching	874.73
-OH	Bending	3437.83
-C-O-	Stretching	1090.65
$-CH_3$	Asymmetric Bending	1454.09
	Symmetric Bending	1430.25
	Asymmetric Stretching	2996.68
	Symmetric Stretching	2921.69
-C=O-	Symmetric Bending	1636.30
-C=O	Carbonyl Stretching	1756.64
-CH-	Symmetric bending	2500
	Asymmetric bending	2851.79
-CH-	Symmetric bending deformation	1386.29
	Asymmetric bending deformation	1365
C=C	Stretching	1590.02

Preprints (www.preprints.org) | NOT PEER-REVIEWED | Posted: 23 September 2020 doi:10.20944/preprints202009.0528.v1

2.3.2 PLA in wired form

PLA wired(filament) form does depict similar peak regions as of granules with slight variation in wavelength. The region shown in figure 10 with hydroxyl group is varied with ±3 cm^{-1}. Table 2 indicate the variation of bonding with type and characteristic peak position study.

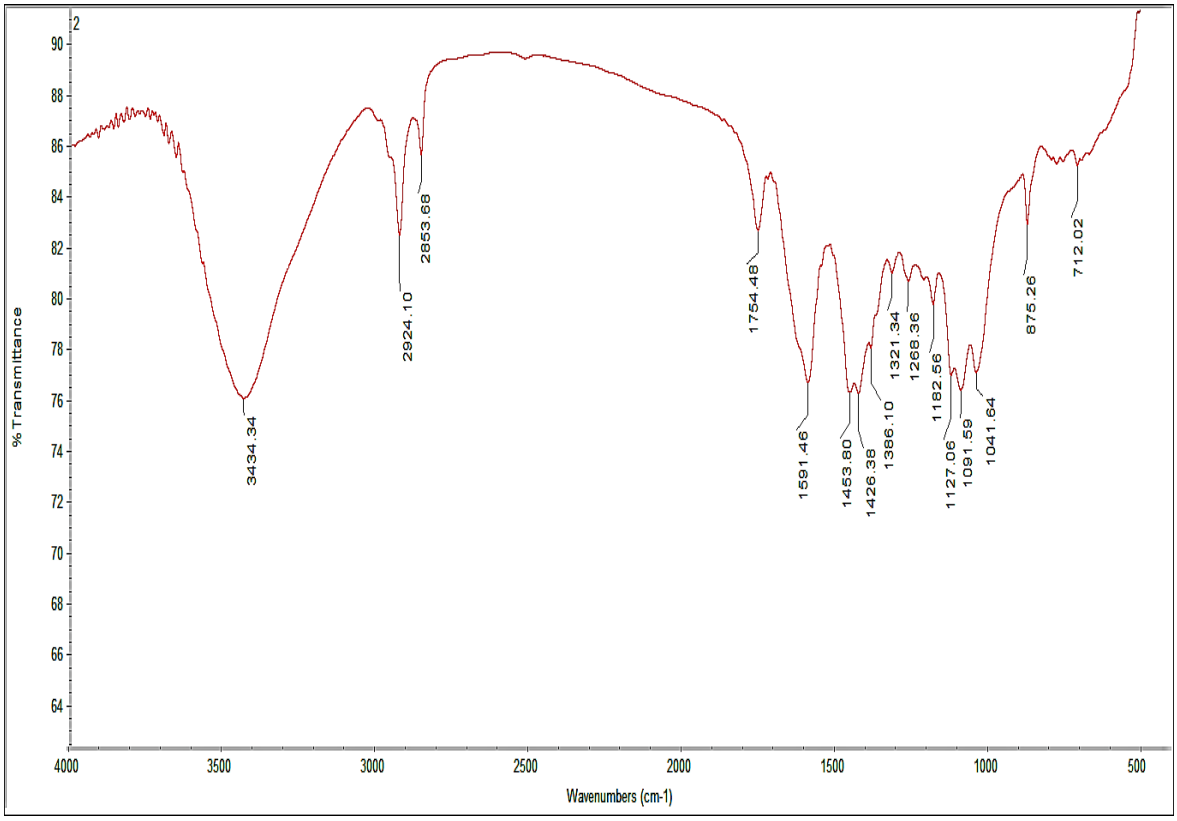

Fig 10. Characteristic bands in IR spectrum of PLA in wired form

Table 2. Characteristic peak positions in IR spectrum for PLA in filament form

Bonding	Type	Characteristic peak positions (cm^{-1})
-C-C-	Stretching	875.26
-OH	Bending	3434.34
-C-O-	Stretching	1091.59
$-CH_3$	Asymmetric Bending	1453.8
	Symmetric Bending	1426.38
-C=O-	Symmetric Bending	1591.46
-C=O	Carbonyl Stretching	1754.48

Preprints (www.preprints.org) | NOT PEER-REVIEWED | Posted: 23 September 2020 doi:10.20944/preprints202009.0528.v1

-CH-	Symmetric bending	2853.68
	Asymmetric bending	2924.1
-CH-	Symmetric bending deformation	1386.1
	Asymmetric bending deformation	1360

2.3.3 Reacted layer on PLA granules

This particular model, subjected to a combination of PLA and concrete hydration or calcinations process due to which the peak of hydroxyl group got shifted as compared to its pristine sample tested for PLA. As the figure 11 shows, symmetric bonding -C=O- shifted from 1591.46(filament PLA) to 1483.96 (reacted PLA) and carbonyl stretching -C=O moved from 1754.48(filament PLA) to 1585.79 (reacted PLA). This indicates a miscibility and interaction taking place between PLA, Cement and fine aggregate. Table 3 depict further clarity on the type, bonding and peak positions of characteristics.

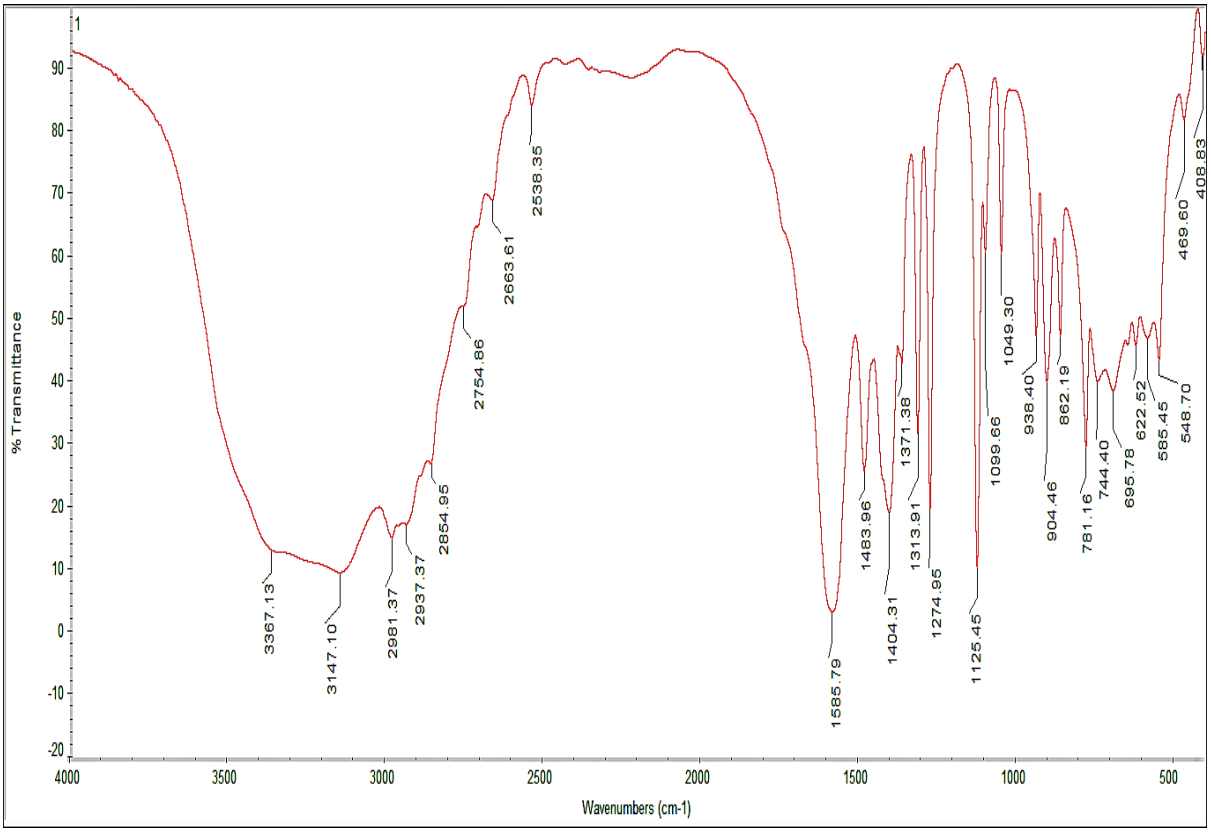

Fig 11. Characteristic bands in IR spectrum of reacted layer on PLA granule

Table 3. Characteristic peak positions in IR spectrum for PLA granules

Bonding	Type	Characteristic peak positions (cm^{-1})
-C-C-	Stretching	781.16

Preprints (www.preprints.org) | NOT PEER-REVIEWED | Posted: 23 September 2020 doi:10.20944/preprints202009.0528.v1

-OH	Bending	3367.13
-C-O-	Stretching	1125.45
$-CH_3$	Asymmetric Bending	1483.96
	Symmetric Bending	1404.31
	Asymmetric Stretching	2981.37
	Symmetric Stretching	2937.37
-C=O-	Symmetric Bending	1483.96
-C=O	Carbonyl Stretching	1585.79
-CH-	Symmetric bending	2754.86
	Asymmetric bending	2854.95
-CH-	Symmetric bending deformation	1404.31
	Asymmetric bending deformation	1371.38

Furthermore, the shift quite naturally due to an interaction between the hydroxyl group of PLA, Cement and water through hydrogen bonding (H-bonding) interaction, resulting in enhanced morphological properties[7].

2.4 Energy-dispersive X-ray Spectroscopy

EDS allows measure/study elemental composition of the specimen. The EDX system may also be able control the SEM scanning system in order to collect elemental distribution maps or elemental line profiles.

In the present study, the samples used for FESEM and EDS are of M20 grade 28 days cured concrete. These tests were conducted on conventional M20 grade concrete and on the concrete where fine aggregate was replaced by PLA granules partially. Replacement levels were 10%, 30% and 50% volume of fine aggregate

2.4.1 Conventional concrete / Concrete without PLA granules

Energy-dispersive spectra obtained from the quantitative elemental analysis on conventional concrete are shown in below figure.

Preprints (www.preprints.org) | NOT PEER-REVIEWED | Posted: 23 September 2020 doi:10.20944/preprints202009.0528.v1

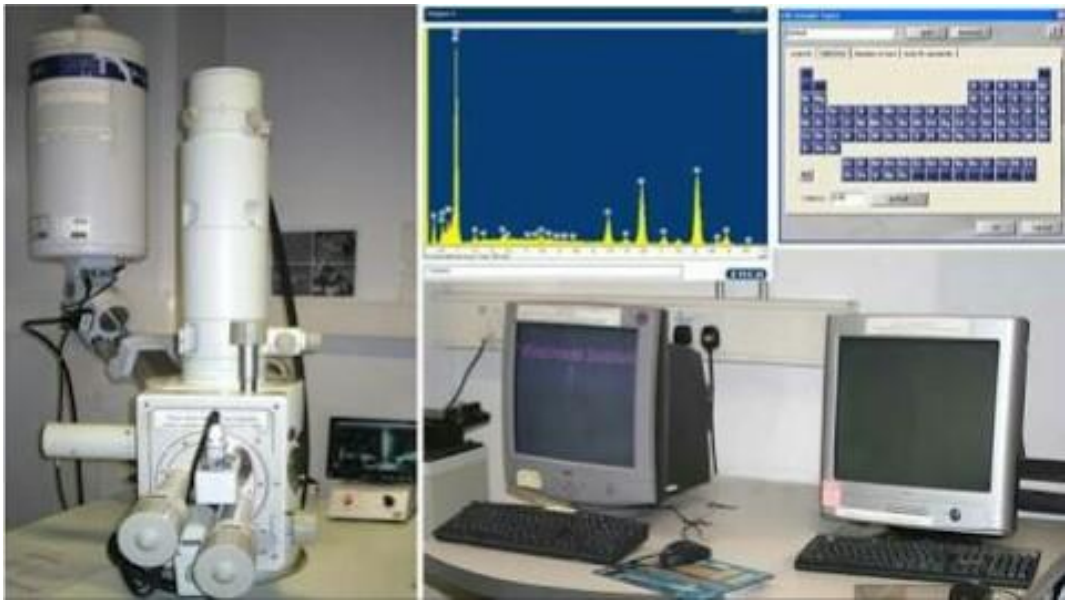

Fig 12. EDX equipment (Courtesy of CMTI, Bangalore)

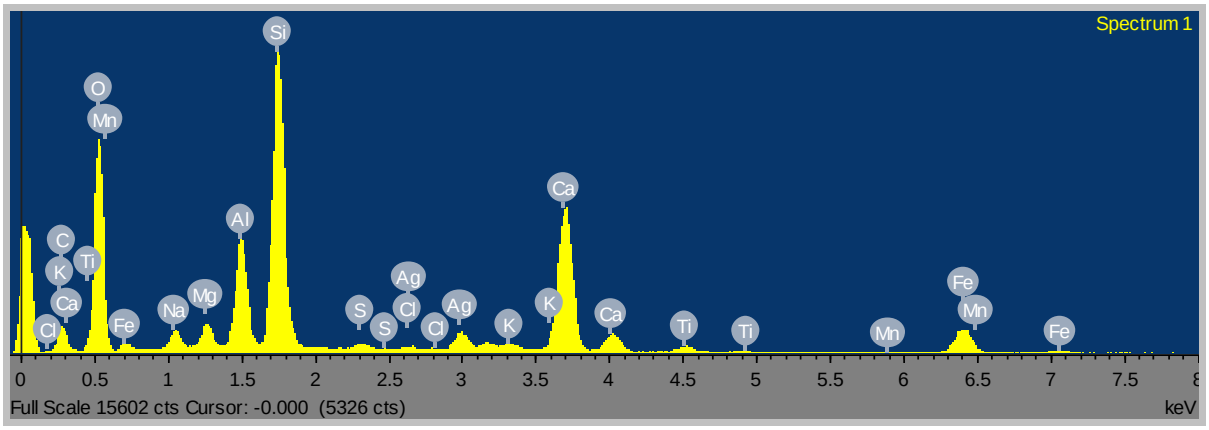

Fig 13. EDX spectrum of conventional concrete

2.4.1.1 10% replacement of fine aggregate by PLA granules

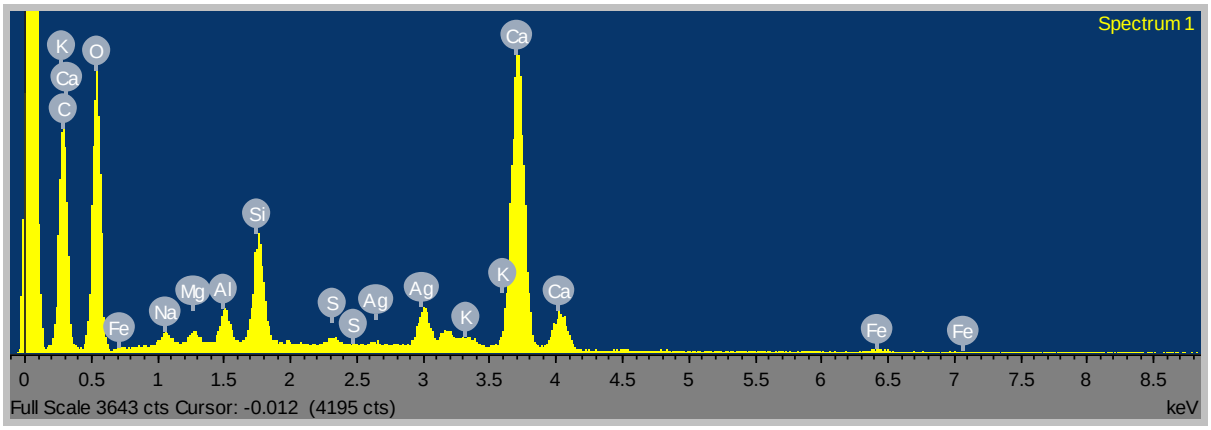

Fig 14. EDX spectrum of 10% PLA used concrete sample

2.4.1.2 30% replacement of fine aggregate by PLA granules

Preprints (www.preprints.org) | NOT PEER-REVIEWED | Posted: 23 September 2020 doi:10.20944/preprints202009.0528.v1

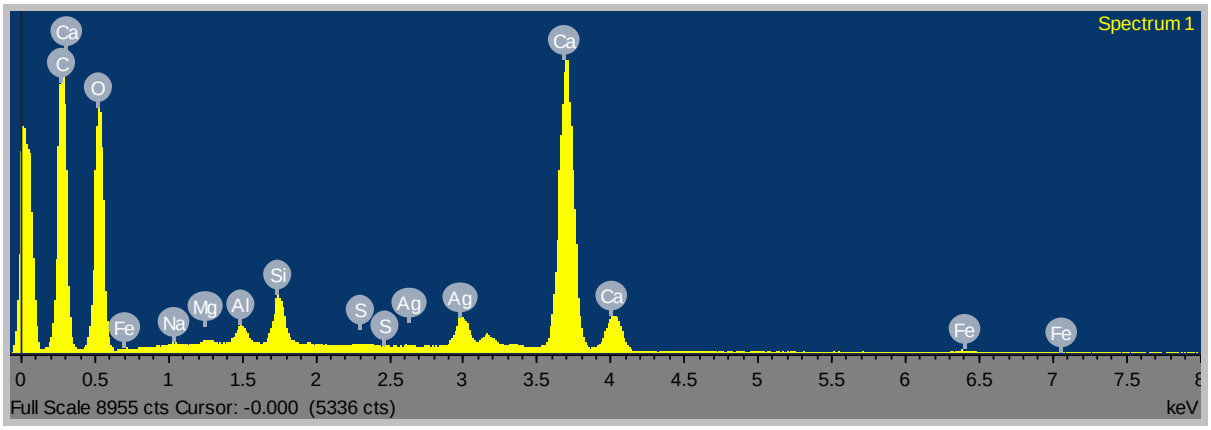

Fig 15. EDX spectrum of 30% PLA used concrete sample

2.4.1.3 50% replacement of fine aggregate by PLA granules

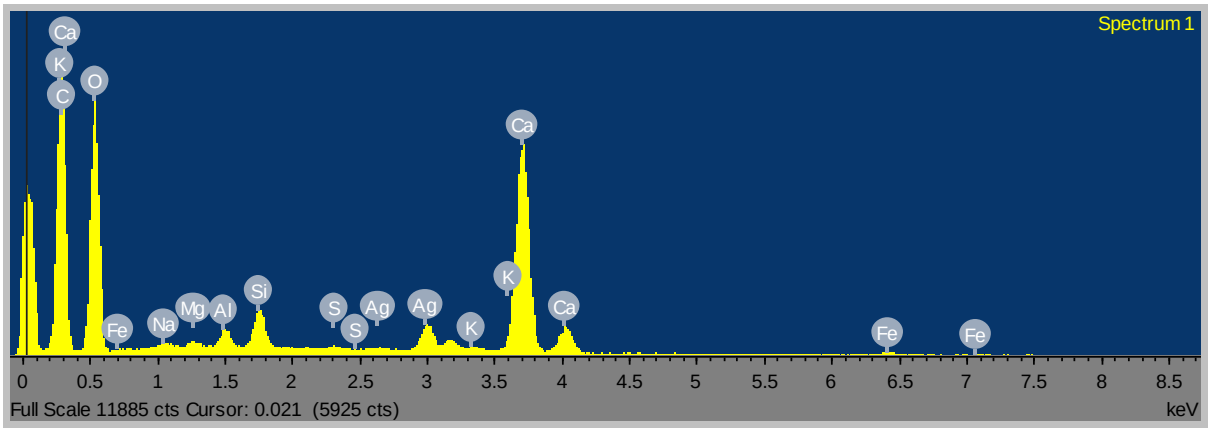

Fig 16. EDX spectrum of 50% PLA used concrete sample

Microscopy observations have been carried out on the fractured and/or flat surfaces of paste samples[6] after 28 days of curing focusing the attention on the bonded area between PLA granules and concrete matrix. Various compounds and elements like $CaCO_3$, SiO_2, Albite (Na), MgO, Al_2O_3, SiO_2, FeS_2 , KCl, Wollastonite(Ca), Ti, Mn and Fe elemental analysis of a sample is tabulated in the Table 4. A unique set of peaks were obtained for each elements atomic structure. In the table 4 higher peaks were observed for Ca. This may be due to the formation of C-S-H gels accelerated by SiO_2 particles. It also indicated the presence of Si, O peaks. The amount of $CaCO_3$ increases with the increase in the percentage replacement of PLA granules. The amount of SiO_2, Albite, MgO decreases due to reduction in the amount of river sand in concrete on its replacement. The amount of Fe, Al_2O_3, MAD-10 Feldspar and FeS_2 decreases with the increase in the percentage replacement of PLA granules due to inert

 doi:10.20944/preprints202009.0528.v1

behaviour of PLA with concrete and reduction in the amount of river sand in concrete on its replacement. The small crystals may be calcium sulfoaluminate, as indicated by the small Sulphur peak in the EDX spectrum[8].

From the table 4, it can be concluded that as the percentage of inclusion of PLA raised from 0 to 10%, calcium carbonate and silica content have raised steeply along with Wollastonite (CaK). From 10 to 30% increase in PLA resulted in further raise of all these elements. Which depicts that concrete mix of cement and coarse aggregate behaves in brittle form and PLA as virgin material behaves brittle in nature, resulting in better mechanical strengths and compared to control concrete mix 30% inclusion results were far more convincing than earlier.

Preprints (www.preprints.org) | NOT PEER-REVIEWED | Posted: 23 September 2020 doi:10.20944/preprints202009.0528.v1

Table 4. EDX spectrum details for 0, 10, 30 and 50% inclusion in concrete as replacement for fine aggregate

X=0			X=10%			X=30%			X=50%		
Element	**Weight (%)**	**Atomic (%)**	**Element**	**Weight (%)**	**Atomic (%)**	**Element**	**Weight (%)**	**Atomic (%)**	**Element**	**Weight (%)**	**Atomic (%)**
C K	5.16	8.36	C K	36.64	46.71	C K	33.98	44.04	C K	41.45	51.00
O K	56.36	68.54	O K	49.42	47.30	O K	51.28	49.89	O K	48.92	45.18
Na K	1.54	1.30	Na K	0.44	0.29	Na K	0.15	0.10	Na K	0.18	0.11
Mg K	1.29	1.03	Mg K	0.29	0.18	Mg K	0.11	0.07	Mg K	0.12	0.07
Al K	4.95	3.57	Al K	0.68	0.39	Al K	0.49	0.28	Al K	0.40	0.22
Si K	14.16	9.81	Si K	2.13	1.16	Si K	1.27	0.70	Si K	0.85	0.45
S K	0.32	0.20	S K	0.16	0.08	S K	0.08	0.04	S K	0.07	0.03
Cl K	0.13	0.07	K K	0.19	0.07	Ca K	12.38	4.81	K K	0.06	0.02
K K	0.34	0.17	Ca K	9.73	3.72	Fe K	0.27	0.07	Ca K	7.72	2.85
Ca K	10.44	5.07	Fe K	0.32	0.09	Totals	100.00		Fe K	0.23	0.06
Ti K	0.57	0.23	Totals	100.00						100.00	
Mn K	0.09	0.03									
Fe K	4.66	1.62									
Totals	100.00										

Preprints (www.preprints.org) | NOT PEER-REVIEWED | Posted: 23 September 2020 doi:10.20944/preprints202009.0528.v1

2.5 Micro-structural study with Scanning Electron Microscopy(SEM)

The entire micro structural study with FESEM plus EDS was carried out at CMTI, Tumkur road, Bangalore. The FESEM images were generated with higher spatial resolution, ultra-precision and accuracy using Carl Zeiss, Sigma 300 VP series model. The detailed study, results and discussion were made in future topics.

2.5.1 Control concrete mix with 0%PLA inclusion

Control concrete mix samples with zero percent PLA inclusion were subjected to micro-structural study, reveal that uniform agglomeration of cement, sand, fine aggregate and coarse aggregate. Figure 17(c) depicts micro cracks observed at fine aggregate removed location.

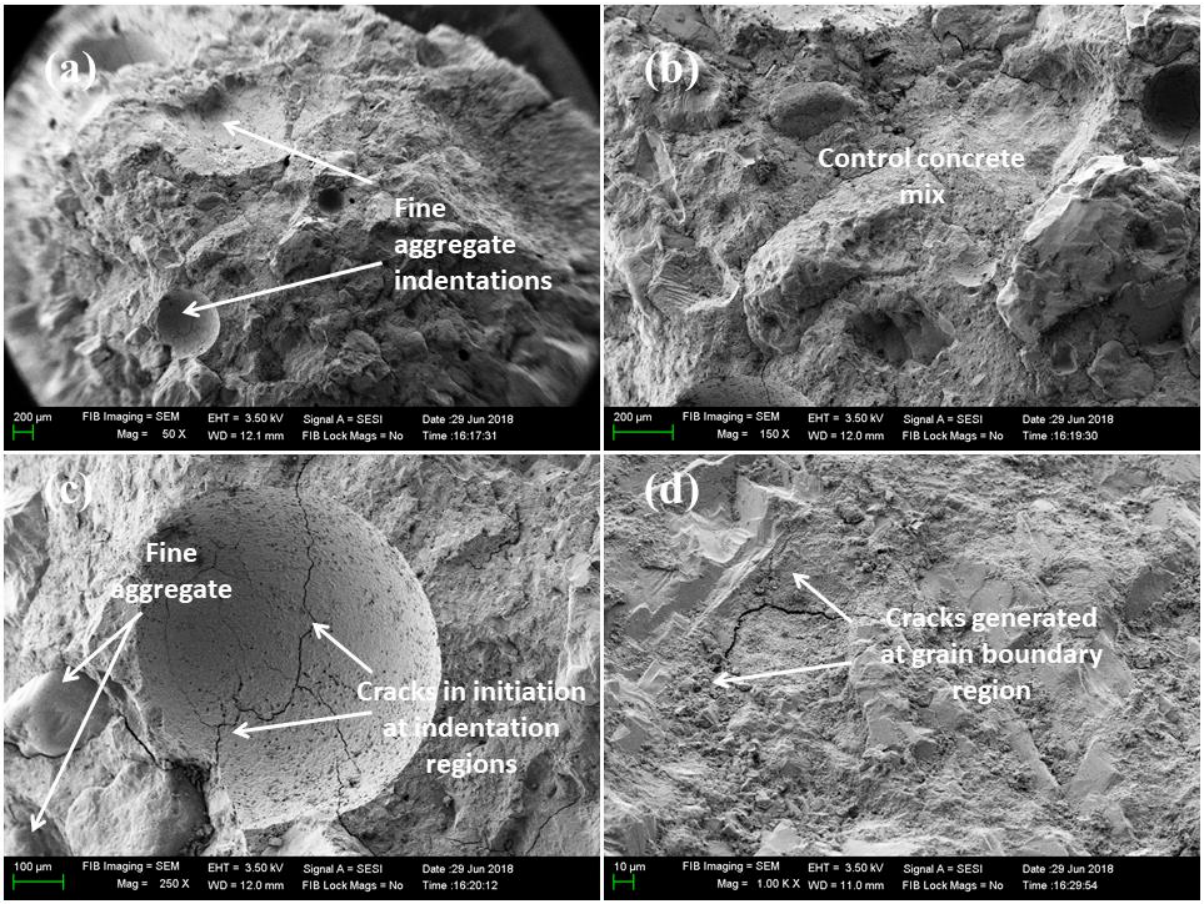

Fig 17. (a-d) Fracture morphology of control concrete mix with 0% inclusion of PLA

Fine aggregates having density of 2.5gm/cc, when casting the control concrete it was found that with PLA inclusion percentages from 0 to 50%, the granules are subjected to movement as they were light in weight(density 1.25gm/cc). This resulted in a top layer becoming more brittle and subjected to higher load bearing capacity. It was clear from figure 18(e-h) that perfect homogeneous blend was arrived with control mix concrete, as fine aggregates were varied in size from 4.75mm down size to till 300µm. Which resulted in air pocket covering at

Preprints (www.preprints.org) | NOT PEER-REVIEWED | Posted: 23 September 2020 doi:10.20944/preprints202009.0528.v1

region were coarse aggregate to cement paste bonding occurred and as cement always go for volume shrinkage it did maintained the bonding even after 28 days of curing.

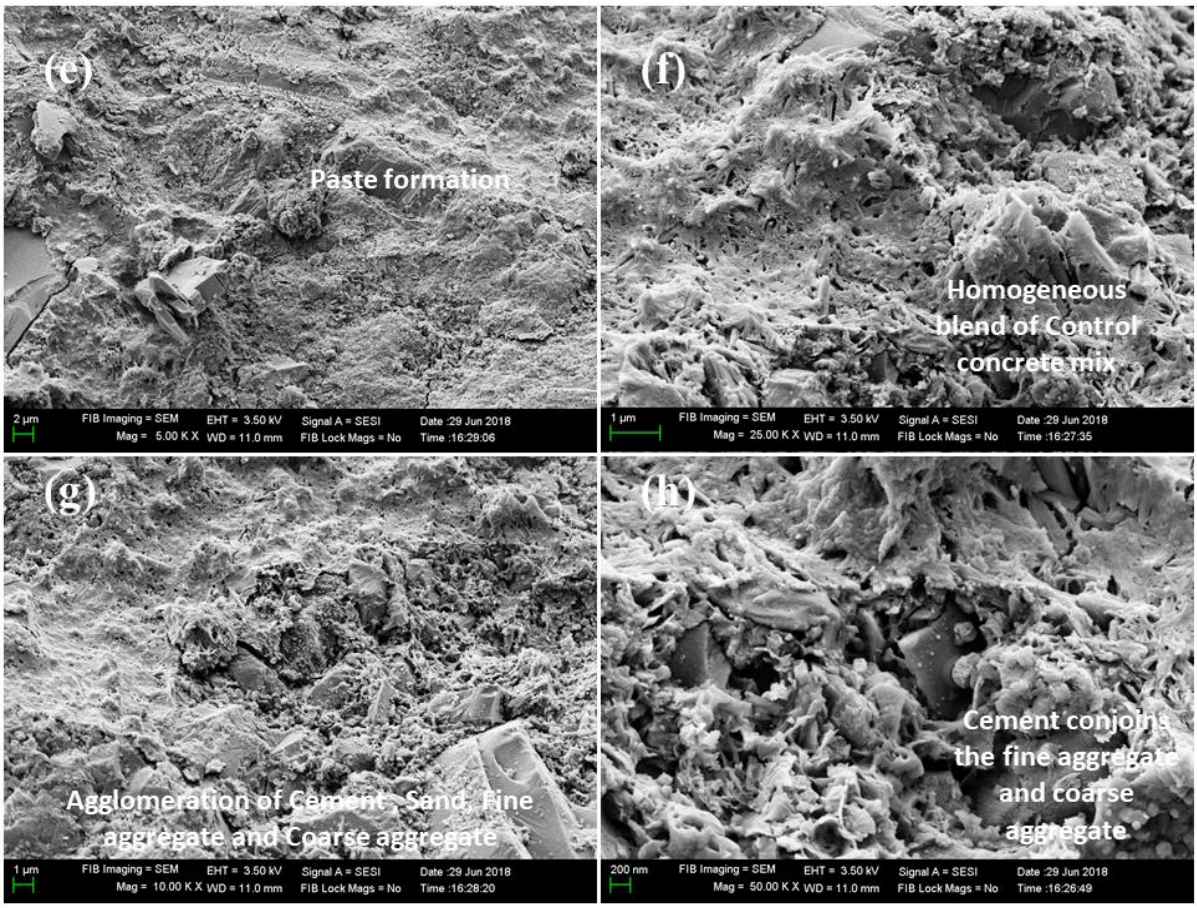

Fig 18. (e-h) Fracture morphology of control concrete mix with 0% inclusion of PLA

2.5.2 With 10%PLA replacement for fine aggregate

From figure 19 (a-d) FESEM images depict the enlarged drawing of the internal structures of PLA and concrete composites. The grain size is calculated by linear intercept method using the formula [9]. The surface morphology of composites changes from dense micro rods to micro-rods interconnected with each other which are randomly oriented along with some flakes and beads with variation of concrete. The micro-rods vary in length and width from 9-11µm and with thickness of 0.2µm for 10% inclusion of PLA. Micro-rod like morphology hindrances due to as content of cement. With Figure 20 (e-h) it can be drawn such as, (e) shows the air pocket inside the PLA granular structure, even being hydrophobic as parent material, when mixed with cement and coarse aggregate, casted and kept for curing at 28 days it did went on to degrade. (f-g) illustrates the bead like structure, these flakes have non uniform lengths showing peaks and valleys in their sizes, providing additional space for inclusion of water and air particles to penetrate into the member and probably allow it for early degradation.

Preprints (www.preprints.org) | NOT PEER-REVIEWED | Posted: 23 September 2020 doi:10.20944/preprints202009.0528.v1

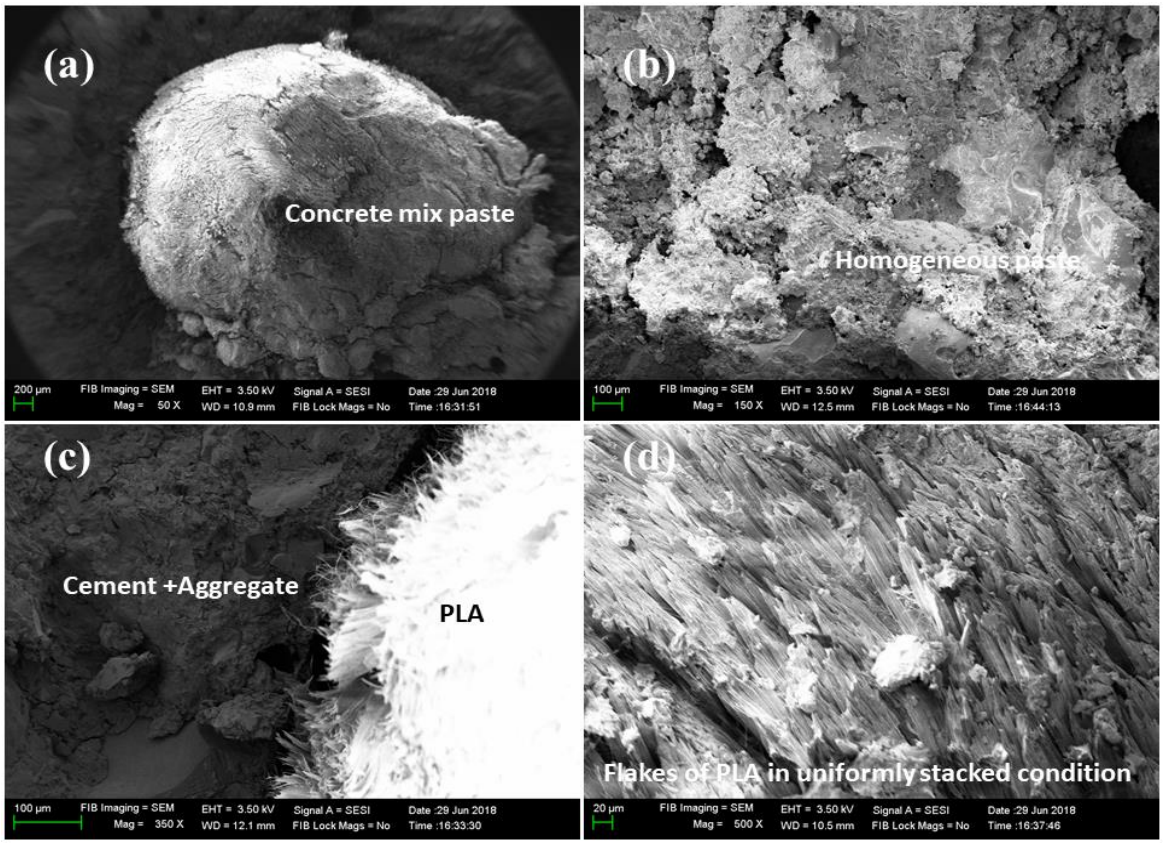

Fig 19. (a-d) Fracture morphology of control concrete mix with 10% inclusion of PLA

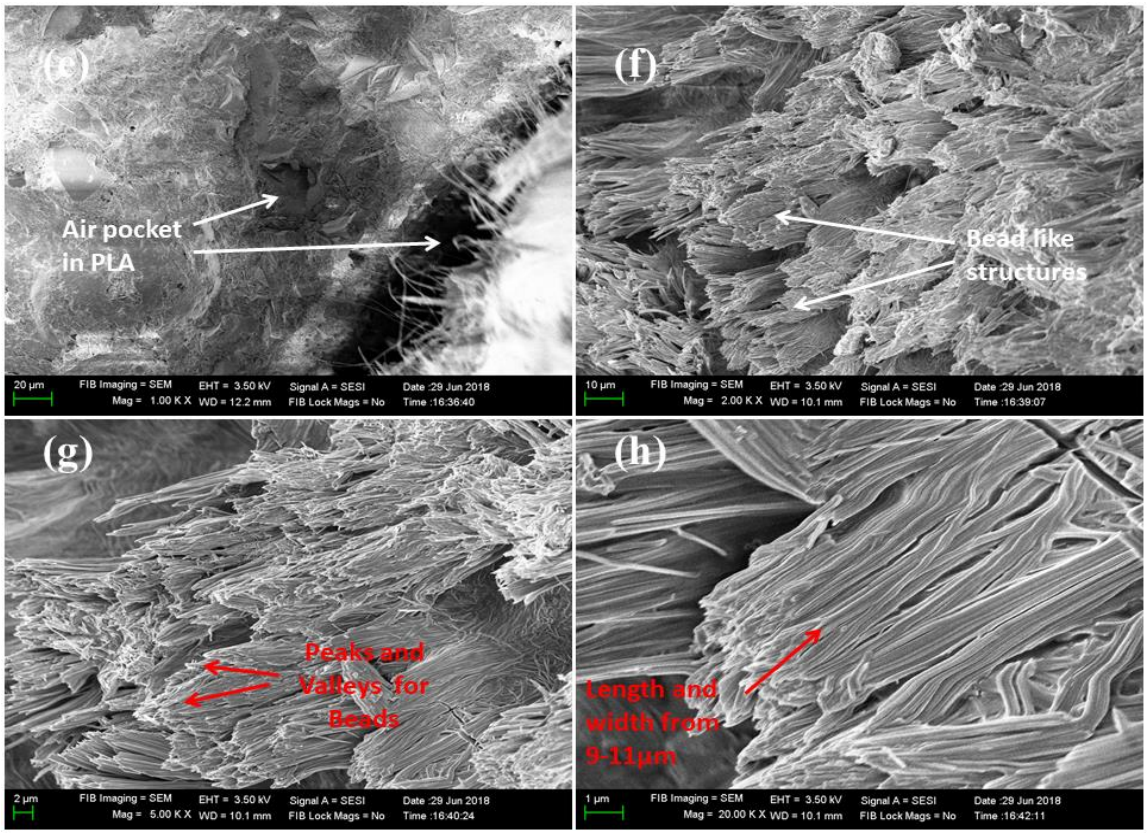

Fig 20. (e-h) Fracture morphology of control concrete mix with 10% inclusion of PLA

Preprints (www.preprints.org) | NOT PEER-REVIEWED | Posted: 23 September 2020 doi:10.20944/preprints202009.0528.v1

2.5.3 With 30%PLA replacement for fine aggregate

The grain size is calculated by linear intercept method using the formula[9] for the sample X=30% inclusion of PLA, the length of rods will have smaller size 5-6µm. As the percentage of PLA inclusion increases in volume when compared to earlier case, there is more provision for free space, because PLA granules are round and glossy shine at the outer face resulting in improper bonding of concrete paste as shown in figure 21(a-d).

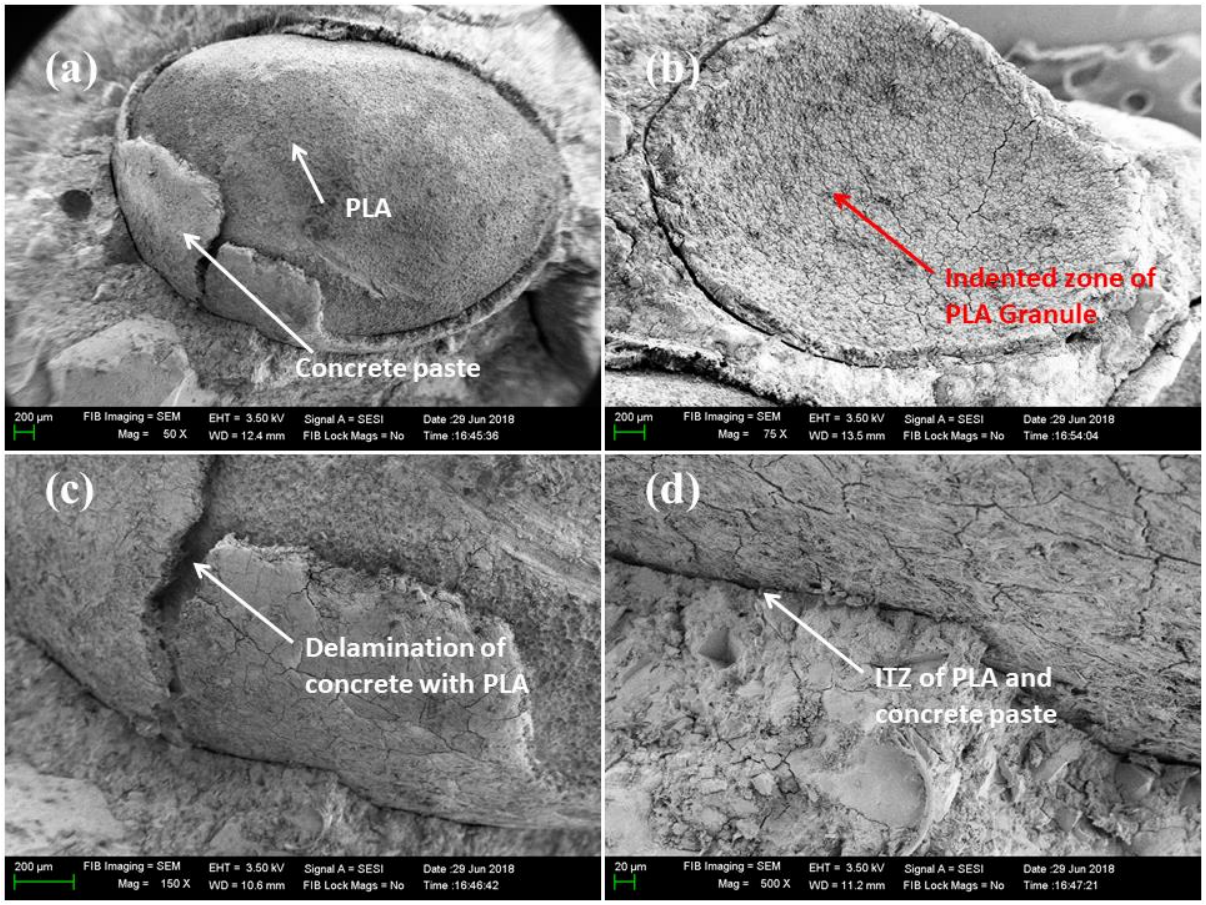

Fig 21. (a-d) Fracture morphology of control concrete mix with 30% inclusion of PLA

From figure 21(d), illustrate about interfacial transition zone (ITZ) between cement paste and PLA. The ITZ can even be extracted from Back Scattered Image(BEI) from SEM machines[10]. Here the work was focused only to identify the ITZ in the SEM images. Fracture behavior will initiate at the outer periphery of PLA, as pristine sample PLA will not break that easily, allow it for transgranular failure pattern. From the data depicts that mechanical tests such compressive strength, flexural strength, split tension test, impact test reveal that 10% inclusion of PLA was far more superior in strength than 30% inclusion[11]. Form figure 22(e-k) it can be concluded that debonding region got enhanced in figure (e) due to continuous loading, stresses generated at the intermediate region, this led to micro crack initiation at the grain boundary regions. As figure(j) depicts the intensification of cracks.

Preprints (www.preprints.org) | NOT PEER-REVIEWED | Posted: 23 September 2020 doi:10.20944/preprints202009.0528.v1

When PLA inclusion percentage increased from 10 to 30, cement became the major filling agent for void or air pocket regions. The behavior resulted in brittle fracture, through SEM images it showed numerous weak zones. Due to debonding fiber channels were visible with large pockets. Pull outs were also visible in all the directions.

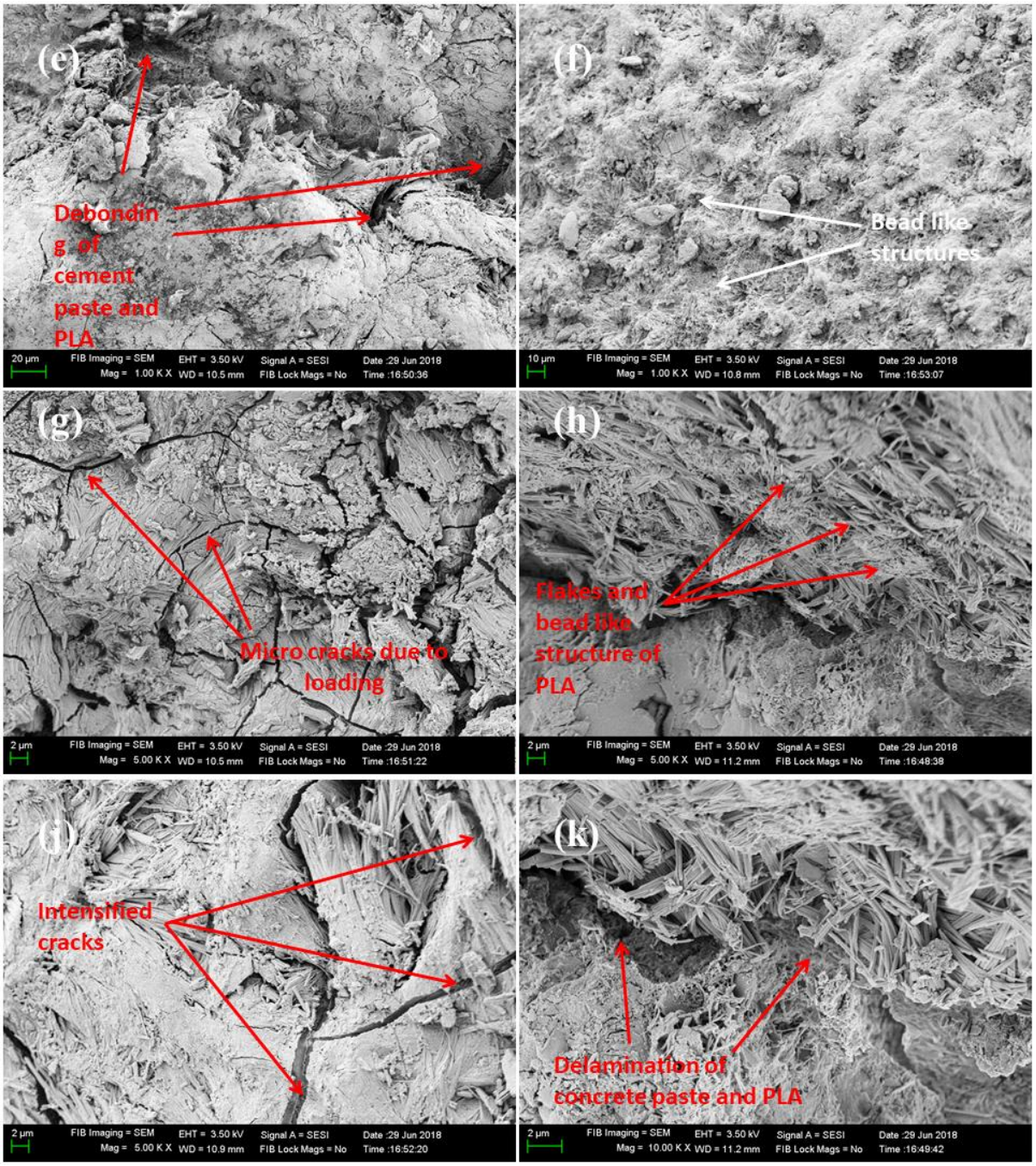

Fig 22. (e-k) Fracture morphology of control concrete mix with 30% inclusion of PLA

2.5.4 With 50%PLA replacement for fine aggregate

From figure 23(a-d) representing similar images as mentioned in case of 30% inclusion of PLA in concrete matrix. As the percentage of PLA inclusion increased, resulting in less gradation of granular sizes, in turn causing more open cavities, less cement and coarse

Preprints (www.preprints.org) | NOT PEER-REVIEWED | Posted: 23 September 2020 doi:10.20944/preprints202009.0528.v1

aggregate mixture, less bonding with PLA granules and finally, outcome shows lowered mechanical strength.

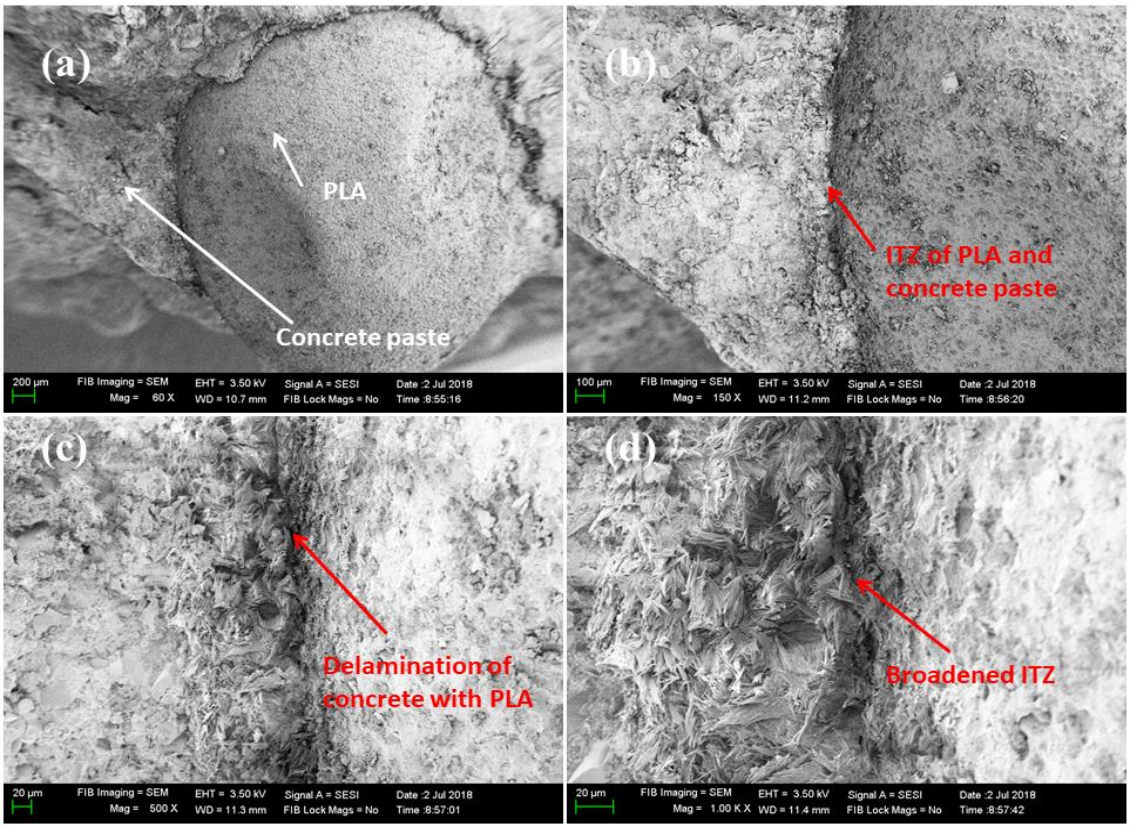

Fig 23. (a-d) Fracture morphology of control concrete mix with 50% inclusion of PLA

From figure 24(e-h), lot more issues related to weak regions in the entire matrix resulting in early failure, and as 50% yielded with higher degradation rate than its lower inclusion rates. The strengths dipped to all time low rate for flexural and impact in comparison to controlled concrete and its successive cases. In case of compressive strength, maximum load will be bear by PLA granules and are really hard to break into pieces. The combination suites not so well for split tension test, as it is subjected to loading, results in early debonding of granules of PLA to cement paste. When external load goes beyond elastic limit of constituent materials in a matrix, results in micro crack and in turn crack deflection will be attained, slowly debonding initiates and rupture of the coupons will be observed.

Preprints (www.preprints.org) | NOT PEER-REVIEWED | Posted: 23 September 2020 doi:10.20944/preprints202009.0528.v1

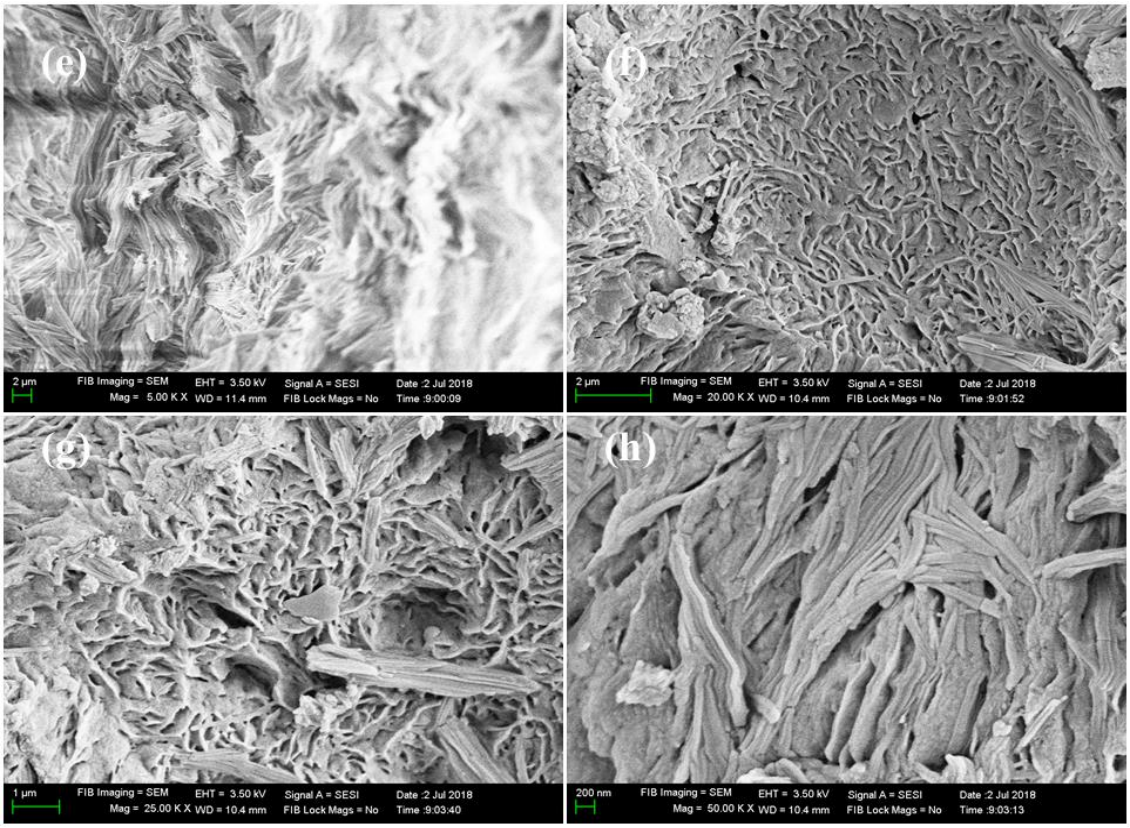

Fig 24. (e-h) Fracture morphology of control concrete mix with 50% inclusion of PLA

3. Conclusion

The exhaustive bio composite characterization resulted in following notable salient points.

1. Thermo gravimetric analysis revealed that PLA either in granular form or filament will hold good for the inclusion into construction applications, provided degradation aspects are to be looked out for improvisation.

2. From DSC it was found that PLA in filament form is the best inclusion material for construction application, however the tenacity of fibers has to checked, as currently available filaments in market does not have high tenacity value.

3. From EDX reports, 30% inclusion of PLA as replacement for fine aggregate has constituent members as Calcium carbonate($CaCO_3$), Silica(SiO_2) and Wollastonite (CaK) resulted in best composition among the rest.

4. Micro-structural study revealed that, proper gradation in size, rough surface of PLA granular form or filament form will definitely enhance the mechanical/physical or even

chemical behavior of PLA. On the other hand degradation is another critical issue with existing biomaterials, So with help of physical vapor deposition (PVD) method a hydrophobic and biocompatible chemical can be coated on the outer periphery of filament or granular form.

Acknowledgement

This work has been partially supported by KLE Technological University, under Research and Development funding project. The author was grateful to Prof. Prakash G Tewari, for his valuable support, Registrar Prof. B L Desai and Vice chancellor Prof. Ashok Shettar for their continuous support. CMTI, Tumkur Road, Bangalore for access to laboratory equipment and facilities, and finally, the author would like to thank reviewers for their helpful comments to improve the quality of this paper.

References

[1]. Statistical Data report from Plastic insight, https://www.plasticsinsight.com/resin-intelligence/resin-prices/polylactic-acid.

[2]. World consumption of lactic acid in 2015, IHS Report.

[3]. Boparai, K.S., R. Singh, F. Fabbrocino, and F. Fraternali. "Thermal characterization of recycled polymer for additive manufacturing applications", *Composites Part B Engineering*, 2016.

[4]. S Salim, H Agusnar, B Wirjosentono, Tamrin, H Marpaung, T Rihayat, Nurhanifa and Adriana, Synthesis and innovation of PLA/clay nanocomposite characterization againts to mechanical and thermal properties, IOP Conf. Series: Materials Science and Engineering 334, 012047, 2018.

[5]. Rihayat, T., Suryani, S., Zaimahwati, Z. 2014. Effects of heat treatment on the properties of polyurethane/clay nanocomposites paint. *Applied Mechanics and Materials*. **525**, 97-100.

[6]. M. Barczewski, D. Matykiewicz, A. Krygier, J. Andrzejewski, K. Skórczewska. "Characterization of poly(lactic acid) biocomposites filled with chestnut shell waste", *Journal of Material Cycles and Waste Management*, 2017.

[7]. Siti Hasnah Kamarudin, Luqman Chuah Abdullah, Min Min Aung, Chantara Thevy Ratnam and Emiliana Rose JusohTalib, A study of mechanical and morphological

 doi:10.20944/preprints202009.0528.v1

properties of PLA based biocomposites prepared with EJO vegetable oil based plasticiser and kenaf fibres, Mater. Res. Express 5, 085314, 2018.

[8]. M.C. Bignozzi, A. Saccani, L. Barbieri, I. Lancellotti. "Glass waste as supplementary cementing materials: The effects of glass chemical composition", *Cement and Concrete Composites*, 2015.

[9]. Shayan, A.. "Performance of glass powder as a pozzolanic material in concrete: A field trial on concrete slabs", *Cement and Concrete Research*, 200603.

[10]. Dalawai, S P, T J Shinde, A B Gadkari, and P N Vasambekar. "Structural properties of Cd–Co ferrites", *Bulletin of Materials Science*, 2013.

[11]. G. Bonifazi, G. C apobianco, S. Serranti, M. Eggimann, E. Wagner, "The ITZ in concrete with natural and recycled aggregates: Study of microstructures based on image and SEM analysis", *15th Euro seminar on Microscopy Applied to Building Materials* 17-19 June 2015 Delft, The Netherland.